The caudal ganglionic eminence is a source of distinct cortical and subcortical cell populations

Susana Nery, Gord Fishell and Joshua G. Corbin

Developmental Genetics Program and the Department of Cell Biology, The Skirball Institute of Biomolecular Medicine, New York University Medical Center, 540 First Avenue, New York, New York 10016, USA

Correspondence should be addressed to G.F. (fishell@saturn.med.nyu.edu)

Published online 4 November 2002; doi:10.1038/nn971

During development, the mammalian ventral telencephalon is comprised of three major proliferative zones: the medial (MGE), lateral (LGE) and caudal (CGE) ganglionic eminences. Through gene expression studies, *in vitro* migration assays, genetic mutant analysis and *in vivo* fate mapping in mice, we found that the CGE is a progenitor region that is distinct from both the MGE and LGE. Notably, CGE cells showed a unique *in vivo* pattern of migration, and the CGE contributed cells to nuclei distinct from those populated by the MGE and LGE. Moreover, we report that the migratory fate of cells from the CGE is intrinsically determined by embryonic day 13.5 (E13.5). Together, these results provide the first insights into the development and fate of the CGE.

The embryonic telencephalon can be broadly subdivided into the cortex and hippocampus dorsally, and the MGE, LGE and CGE ventrally. Determining how these embryonic structures give rise to those found in the mature brain is a key to understanding telencephalic development. Currently, much is known about the development and fate of cells born in the MGE and LGE. Although the CGE represents approximately 40% of the E13.5 ventral telencephalon, little is known about the developmental fate of this region. Defined as the region posterior to where the MGE and LGE fuse into a single structure, it is presently unclear whether the CGE is a posterior extension of the MGE or the LGE, a combination of both, or a unique structure.

In mice, our understanding of the development and fate of the MGE and LGE has come from a number of distinct approaches including (i) inferences based on morphology (such as comparison of embryonic versus adult topography)[1,2], (ii) analysis of gene expression patterns during development[3], (iii) *in vitro* migratory assays using lipophilic dye labeling[4–9] and (iv) analysis of mutant mice lacking genes that affect these structures[10–16]. Taken together, these studies suggested that the MGE and LGE give rise to the basal ganglia (striatum and globus pallidus) and, via tangential migration, are also a source of the majority of interneurons in the cerebral cortex, hippocampus and olfactory bulb[17,18]. These structures are also thought to be a significant source of oligodendrocytes[19–23].

We have developed a method in which ultrasound backscatter microscopy (UBM)-guided homotopic transplantation can be used to fate-map the MGE and the LGE[24]. This previous study provided the first *in vivo* evidence that MGE cells largely migrate to the cortex, where they differentiate into interneurons. This study also confirmed *in vivo* that the LGE mainly gives rise to the projection neurons of the striatum[25] and interneurons of the olfactory bulb.

In the present study, we examined the CGE at E13.5. Although the CGE shares the expression of certain markers with the LGE or the MGE, gene expression in the CGE matches neither region completely. Furthermore, mutations in *Titf1* (also known as *Nkx2.1*) or *Gsh2*, which affect the MGE and LGE, respectively, did not result in changes in gene expression in the CGE or in the ability of CGE-derived cells to migrate *in vitro*. Most strikingly, our *in vivo* homotopic transplantation experiments revealed that CGE-derived cells have a characteristic pattern of migration and contribute to a number of mature structures in the adult brain. These include layer-5 neurons of the cerebral cortex, as well as the striatum and specific regions of the limbic system. Moreover, heterotopic transplantation of MGE cells into the CGE revealed that intrinsic character rather than inductive local cues underlie migratory differences between the ventral eminences. Taken together, these results show that the CGE has several properties that are distinct from both the MGE and LGE, and is an important region for contributing cells to numerous brain structures.

Results

Molecular characterization of the CGE

Several genes, such as *Dlx2*, *Titf1*, *Ascl1* (formerly known as *Mash1*) and *Lhx6*, are expressed in the MGE and the LGE and are involved in the specification of these structures and the generation of interneurons and oligodendrocytes[4,7,10,11,13,14,20]. At E13.5, we found that the transcription factors *Dlx2* and *Ascl1* were expressed in the ventral ganglionic eminences, including the CGE (**Fig. 1a**, **b** and **h**). In contrast, expression of *Neurog2* (also known as *Ngn2*), which encodes Neurogenin 2, was restricted to the dorsal ventricular zone (VZ) and excluded from the CGE (**Fig. 1c** and **i**). *Sfrp2*, which encodes secreted frizzled-related protein 2 (SFRP2), was expressed in cells that border the pallial-subpallial boundary and delineated the CGE from the cortex (**Fig. 1d** and **j**

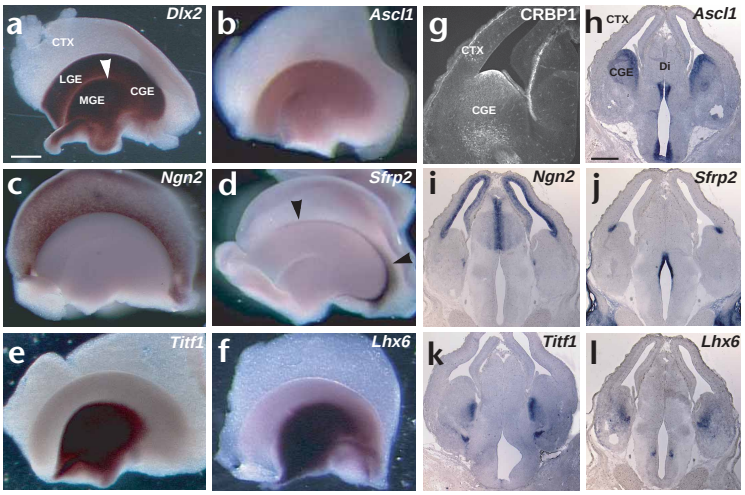

Fig. 1. Molecular characterization of the CGE at E13.5. (**a**–**f**) *In situ* hybridization of whole-mount telencephalic slices and (**h**–**l**) coronal sections, and (**g**) immunofluorescence on coronal sections, revealed that the CGE expresses a unique combination of ventral telencephalic markers. For whole mounts (**a**–**f**), anterior is to the left and posterior to the right. (**a**) *Dlx2* and (**b**, **h**) *Ascl1* were expressed ventrally. Arrowhead in (**a**) shows end of the sulcus separating the MGE from LGE. (**c** and **i**) *Neurog2* (*Ngn2*) expression was mostly restricted to the cortex, and (**d**, **j**) *Sfrp2* was expressed (arrowheads) between the CGE, the LGE, and the overlying cortex. (**e**, **k**) *Titf1* and (**f**, **l**) *Lhx6* were expressed ventrally in the MGE and in the anterior CGE. (**g**) CRBP1 was expressed at high levels in the CGE. CGE, caudal ganglionic eminence; CTX, cortex; Di, diencephalon; LGE, lateral ganglionic eminence; MGE, medial ganglionic eminence. Scale bars, (**a**–**f**) 300 μm, (**g**) 250 μm and (**h**–**l**) 500 μm.

and ref. 26). *Titf1* and *Lhx6* were expressed in the anterior part of the CGE (**Fig. 1e, f, k** and **l**). Notably, the expression of *Lhx6* extended more posteriorly in the CGE than did *Titf1*. Cellular retinol binding protein 1 (CRBP1), in addition to being expressed in the LGE[27], was strongly expressed in the CGE (**Fig. 1g**).

Thus, the CGE shares some molecular markers with both the MGE and the LGE, but is molecularly distinct from each. These criteria suggest that the CGE may be a posterior extension of both the MGE and LGE, or it may have a unique identity.

The CGE is genetically distinct

To determine whether mutations that affect the development of the LGE or the MGE also have a similar effect on the CGE, we analyzed the status of the CGE in the absence of either *Gsh2* or *Titf1*, which results in defects in the LGE and MGE, respectively. Consistent with previous results[12,15,16,28], in the absence of *Gsh2*, expression of *Dlx2* was reduced in the mutant LGE (**Fig. 2a** and **b**), and that of *Neurog2* expanded (**Fig. 2e** and **f**). Notably, in the absence of *Gsh2*, *Dlx2* remained strongly expressed in the CGE (**Fig. 2c** and **d**), and *Neurog2* expression was not expanded (**Fig. 2g** and **h**). These results suggest that the LGE and the CGE are genetically distinct and that the CGE does not simply represent a caudal extension of the LGE.

It has been previously shown that in *Titf1* mutant mice, the MGE is not properly specified, and there is a conversion from MGE to LGE fate[14] with a subsequent loss of expression of *Lhx6* in the mutant MGE (**Fig. 2i** and **j**) and CGE (**Fig. 2k** and **l**). The conversion of the MGE to an LGE fate in the absence of *Titf1* also results in the expansion of striatal markers[14]. Consistent with this expansion, we found that in the absence of *Titf1* gene function, expression of *Ebf1*, which marks developing striatal cells[29], expanded ventrally into the presumptive region of the mutant MGE (**Fig. 2m** and **n**). In contrast, in the CGE, *Ebf1* expression was not affected in animals lacking *Titf1* (**Fig. 2o** and **p**). The lack of transformation of the CGE into an LGE fate suggests that *Titf1* is not required for the specification of the CGE. However, as the anterior-most aspect of the CGE contains both *Titf1* and *Lhx6*, it cannot be ruled out that this region of the CGE is affected by the loss of *Titf1*. As *Lhx6* expression is lost in the *Titf1* mutant in both the MGE and CGE, we further investigated potential differences between these two structures by comparing their *in vitro* migratory potential. VZ and SVZ (subventricular zone) from MGE, LGE, CGE and cortex were dissected (**Fig. 2v** and **w**) from control and *Titf1* mutant E13.5 embryos, and explants were cultured *in vitro* in reconstituted extracellular matrix gel (Matrigel, see Methods) for 1–11 days (**Fig. 2q–u** and data not shown). Consistent with previous studies[20,30], at 3 days *in vitro* (d.i.v.), control MGE cells (**Fig. 2q**) migrated more than LGE cells (**Fig. 2r**), whereas cortical cells extended processes and showed little migration (data not shown and ref. 20). Additionally, CGE cells migrated extensively (**Fig. 2t**). Consistent with the mutant MGE possessing LGE properties, MGE explants from *Titf1* mutant mice showed reduced migratory potential (**Fig. 2s** and ref. 20). Despite the loss of *Titf1* and *Lhx6* in the CGE, however, migration from *Titf1* mutant CGE explants was indistinguishable from control CGE (**Fig. 2u**). Migration at 3 d.i.v. was also quantified, and the results were consistent with the qualitative observations (**Fig. 2x**). Migration from both control MGE ($n = 5$) and control CGE ($n = 6$) explants was greater than that from control LGE ($n = 5$) explants ($P < 0.003$ and $P < 0.002$, respectively). Similar comparison revealed that migration from the mutant *Titf1* MGE ($n = 5$) explants was reduced ($P < 0.02$) compared to control MGE explants and was not significantly different from control LGE ($P = 0.264$). In contrast, the loss of *Titf1* had no effect on migration from CGE explants ($n = 5$, $P = 0.953$). These results suggest that despite the anterior-most region of the CGE sharing marker expression with the MGE (*Titf1* and *Lhx6*), the majority of CGE cells retain the ability to migrate in the absence of *Titf1* gene function.

Dlx2-positive cells migrate extensively from the CGE

Dlx2 is widely expressed throughout the ventral telencephalon and labels tangentially migrating cells to the cortex. Furthermore, the loss of both *Dlx1* and *2*, in addition to having a defect in striatal differentiation, also results in a 75% decrease in the number of cortical interneurons[4]. To study the contribution of the CGE to the tangentially migrating population of *Dlx2* cells, we examined a transgenic line in which the *tau-lacZ* reporter was targeted to the *Dlx2* locus[12]. At E14.5 and E15.5, many *LacZ*-positive cells emanated from the CGE region and migrated to the cortex and hippocampus (**Fig. 3a–d**). At these ages, two major streams of migrating cells were observed, one through the SVZ/lower intermediate zone (IZ) and a second through the marginal zone (MZ). Notably, neither stream of cells overlapped with IZ axons (**Fig. 3c**), suggesting that these cells do not use corticofugal fibers as a substrate for migration. Although *Dlx2* is widely expressed throughout the ventral telencephalon, the large number of

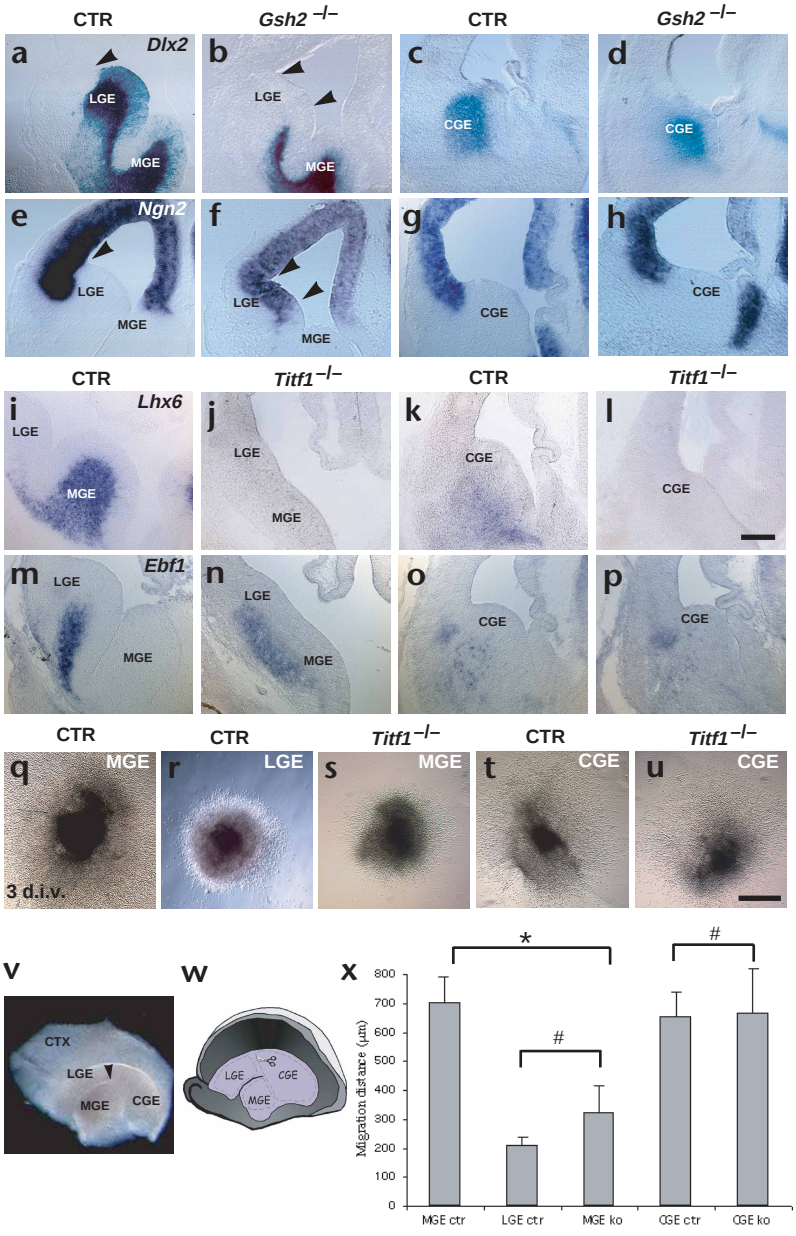

Fig. 2. The CGE is unaffected in the absence of *Gsh2* or *Titf1*. (**a**) In the LGE, the dorsal limit of *Dlx2* expression was near the cortical-striatal sulcus (arrowhead). (**b**) In the absence of *Gsh2*, *Dlx2* expression was lost in most of the LGE (arrowheads). (**c**) *Dlx2* was expressed in the CGE. (**d**) In *Gsh2* mutants, *Dlx2* remained highly expressed in the CGE. (**e**) *Neurog2* (*Ngn2*) expression was normally restricted to the pallium and excluded from the LGE (arrowhead). (**f**) In the absence of *Gsh2* gene function, *Neurog2* expression expanded significantly into the LGE (arrowheads). (**g**) *Neurog2* was not expressed in the CGE. (**h**) In the absence of *Gsh2* gene function, *Neurog2* expression remained excluded from the CGE. *Lhx6* was normally expressed at high levels in the (**i**) MGE and at lower levels in the (**k**) CGE. In the absence of *Titf1* gene function, expression in both the (**j**) MGE and (**l**) CGE was lost. (**m**) *Ebf1* was expressed in the LGE. (**n**) In the absence of *Titf1* gene function, *Ebf1* expression extended into the mutant MGE. (**o**) *Ebf1* was expressed only in a subset of cells in the CGE. (**p**) In the absence of *Titf1* gene function, the domain of *Ebf1* expression did not expand in the CGE. For analysis of cell migration, explants from the indicated regions were cultured *in vitro* for (**q**–**u**) 3 d.i.v. (**v**) Whole mount view an E13.5 telencephalic sagittal slice indicating the MGE, LGE and CGE and (**w**) a schematic of the dissected regions. Arrowhead (**v**) shows the posterior extent of the sulcus separating the MGE from the LGE and the beginning of the CGE. Cells from control (**q**, **x**) MGE and (**t**, **x**) CGE displayed extensive migration away from the core of the explant. In contrast, cells from control (**r**, **x**) LGE explants exhibited little migration. Cells from (**s** and **x**) MGE explants from animals lacking *Titf1* gene function migrated significantly less than controls ($^{*}P < 0.02$) and displayed a level of migration that is not significantly different from that of LGE explants ($^{\#}P = 0.264$). In contrast, migration from (**u**, **x**) CGE explants derived from *Titf1* mutant animals was not significantly affected ($^{\#}P = 0.953$). (**x**) Quantification of the distance of cell migration (μm) away from the edge of each explant at 3 d.i.v. Error bars show standard error. Scale bars, (**a**–**p**) 250 μm; (**q**–**u**) 500 μm.

Dlx2-tau-lacZ–positive cells apparently emanating from the CGE suggests that this structure may be a source of cells migrating tangentially to the cortex and hippocampus.

CGE cells are highly migratory *in vivo*

To investigate the migratory potential and fate of CGE progenitors *in vivo*, cells were transplanted from donors that constitutively express alkaline phosphatase to wild-type hosts at E13.5 using UBM-guided microscopy (**Fig. 4a** and **f**). Four days after homotopic transplantation ($n = 6$ brains), CGE-derived cells migrated extensively from the site of transplantation to the developing neocortex and hippocampus, but mainly at posterior levels (**Fig. 4b–e**). At this time point, however, many cells remained in the CGE near the site of transplantation. Results from age-matched MGE transplants were similar ($n = 4$ brains), with the exception that fewer cells migrated to the hippocampus (**Fig. 4g–j** and ref. 24). In contrast, homotopically transplanted LGE cells ($n = 2$ brains) did not migrate to the cortex but instead migrated ventrally, and primarily remained within the striatum (**Fig. 4k–n** and ref. 24). Thus, CGE-grafted cells migrate extensively *in vivo*, contributing cells to the cortex and hippocampus.

CGE-derived cells contribute to distinct nuclei

To examine the final location and fate of CGE-derived cells, animals receiving homotopically transplanted cells at E13.5 were analyzed at postnatal day (P) 21 ($n = 8$ brains). CGE cells were found to contribute to numerous brain structures (**Figs. 5a–f** and **6a**, **d**, **f**, **h**, **j**; **Supplementary Fig. 1c, d,** and **j–n** online; summarized in **Supplementary Table 1** online). The following were the most striking findings: CGE cells migrated to the cortex, especially at more caudal levels, where they differentiated into neurons that almost exclusively populated layer 5 (**Figs. 5a–i** and **6h**). CGE-derived cells also contributed to numerous structures of the limbic system, including the posterior nucleus accumbens (NAc) (**Fig. 5a**), the bed nucleus of the stria terminalis (BNST) (**Fig. 5b**), the hippocampus (**Figs. 5c–f** and **6d**, **f**) and specific

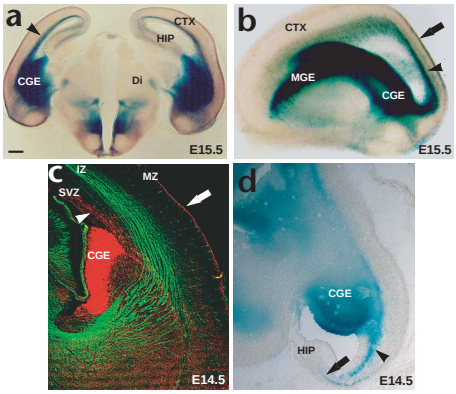

Fig. 3. *Dlx2-tau-LacZ* knock-in mouse allows visualization of *Dlx2* expression and significant migration of *Dlx2* positive cells from the CGE at E14.5 and E15.5. (**a**, **b**, **d**) X-gal stained (**a**) coronal, (**b**) sagittal and (**d**) horizontal sections show expression of *Dlx2* in the MGE, LGE and CGE and putative streams of migrating cells (MZ, arrows; SVZ, arrowheads) from the CGE to the cortex and hippocampus. (**c**) Double immunofluorescence performed on coronal sections reveals β-galactosidase expressing cells possibly migrating from the CGE to the cortex (red) through the SVZ (arrowhead), not overlapping with neurofilament-145 that labels the intermediate zone corticofugal fibers (green). A stream of cells is also observed migrating through MZ (arrow). HIP, hippocampus; IZ, intermediate zone; MZ, marginal zone; SVZ, subventricular zone. Scale bars, (**a**) 250 μm, (**b**) 450 μm, (**c**) 50 μm and (**d**) 125 μm.

nuclei of the amygdala (**Figs. 5c–f** and **6j**). In addition, CGE cells populated the posterior striatum and, to a lesser extent, the posterior globus pallidus (**Fig. 5c** and **d**; **Supplementary Fig. 1j–n**).

CGE-derived cells and axonal projections were also found in other regions of the brain such as the olfactory nucleus, the piriform cortex and ventral pallidum (**Fig. 5a–c** and **Supplementary Fig. 1c**). In the septum, axonal projections were seen (data not shown), but cells were found only in some of the brains receiving transplants (**Fig. 5a**). Axonal projections originated from the striatum and globus pallidus and terminated in the lateral pars reticulata and pars compacta of the substantia nigra (SN). The amygdala may be another source of the fibers seen in the pars compacta of the SN (**Fig. 5e** and **f**). In addition, we found fibers in the stria terminalis and in the CA1 and dentate gyrus of the hippocampus (**Figs. 5c–f** and **6d**, **f**). In contrast, only a few cells were observed in the olfactory tubercle, anterior striatum, anterior NAc or anterior globus pallidus (**Fig. 5a** and **b**; **Supplementary Fig. 1j–n**). In summary, this fate-map analysis indicates that the E13.5 CGE contributes to numerous regions of both the dorsal and ventral brain. Notably, the CGE contributes cells to layer 5 of the cortex, specific regions of the limbic system (amygdala, hippocampus and NAc) and the striatum.

Several cell types were identified on the basis of their cellular morphology ($n = 11$). In the cerebral cortex, most of the cells had a stellate interneuronal morphology (**Fig. 5i–k**), and a minority of these cells had an ascending projection to the MZ (**Fig. 5j**). Although the majority of the cells were present in layer 5 (**Fig. 5g–k**), we also found cells in the marginal zone (MZ) and a few in more superficial layers (data not shown). There were very few oligodendrocytes or astrocytes in the cerebral cortex. In the hippocampus, a variety of cell morphologies could be seen, including small spindly interneurons (**Fig. 5l**), mossy cells (**Fig. 5m**), and a few pyramidal and granule cells (**Fig. 5n** and data not shown). The majority of the cells in the striatum were medium spiny projection neurons (**Fig. 5o**), but aspiny neurons were also present in smaller numbers (data not shown). A large number of oligodendrocytes and astrocytes were also observed in the striatum. In the posterior globus pallidus, there were a few medium spiny and aspiny neurons. Other morphologies included medium aspiny neurons in the amygdala (**Fig. 5p**) and neurons resembling ChAT cells located in the septum and nucleus accumbens (**Fig. 5q**). Oligodendrocytes and astrocytes were also observed in the piriform cortex (data not shown). In summary, the CGE-derived cells resemble interneurons, inhibitory projection neurons and glia.

Additionally, we compared the final fate and localization of cells derived from each of the ganglionic eminences (**Supplementary Table 1**, **Fig. 6** and **Supplementary Fig. 1**). The CGE contributed a large number of cells to the posterior but not the anterior NAc (**Fig. 6a**). In contrast, the LGE mainly supplied cells to the anterior NAc (**Fig. 6c**). Hence in the NAc, CGE and LGE-derived cells were complementary in their distribution. Conversely, few MGE-derived cells were seen in this structure (**Fig. 6b**). CGE-derived cells also migrated to the hippocampus at both anterior and posterior levels with the majority of the cells located both in CA1 and CA3, suggesting that the CGE

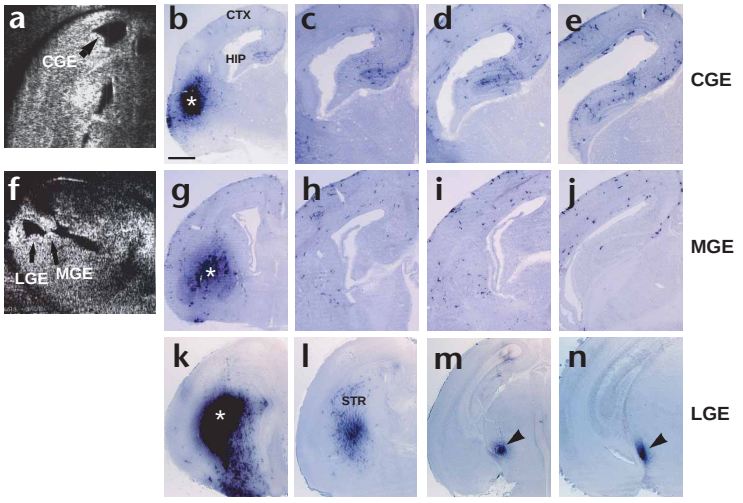

Fig. 4. *In vivo* assays show that CGE cells are highly migratory at E13.5. (**a** and **f**) UBM images showing coronal views of E13.5 brains at the (**a**) CGE level and more anterior at the (**f**) MGE/LGE level. Arrows show the targeted site for transplantation. (**b–n**) Coronal views of anterior to posterior distribution of (**b–e**) CGE, (**g–j**) MGE and (**k–n**) LGE cells four days after homotopic transplantation of cells expressing alkaline phosphatase (E17.5). (**b–e**) Four days after transplantation, many CGE grafted cells were detected around the injection site (asterisk), but numerous CGE cells migrated to the cortex and hippocampus, especially at posterior levels. (**g–j**) Tangential migration from the ventral telencephalon to the cortex is also seen in the MGE transplants. (**k–n**) On the contrary, LGE-derived cells did not migrate to the cortex, but instead dispersed within the ventral telencephalon, mainly in the striatum. (**m**, **n**) In LGE transplants, projections to the substantia nigra are also observed (arrowheads). STR, striatum. Scale bar (**b–e** and **g–n**), 300 μm.

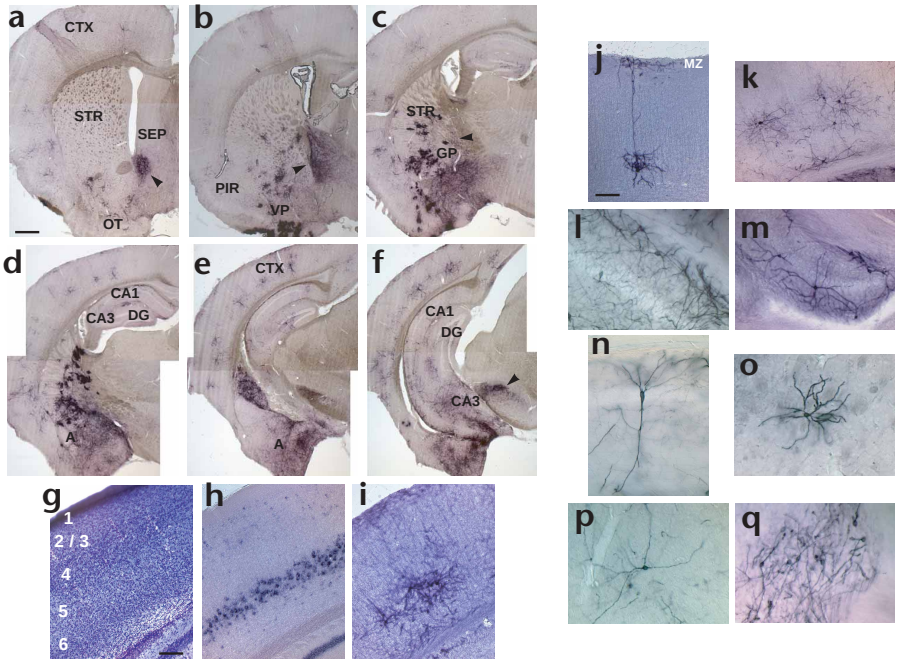

Fig. 5. Distribution and morphology of CGE-derived cells at P21. (**a**–**f**) Anterior to posterior coronal sections of a P21 brain grafted with CGE cells at E13.5 expressing alkaline phosphatase. CGE-derived cells migrate to and differentiate mainly in the (**a**) posterior nucleus accumbens (arrowhead), (**b**) bed nucleus of stria terminalis (arrowhead) and (**c**) posterior striatum (STR) and globus pallidus (GP); fibers in the stria terminalis are also shown (arrowhead). (**d**–**f**) Specific nuclei of the amygdala, (**c**–**f**) hippocampus and (**a**–**f**) cortex, especially at posterior levels. (**g**–**i**) In the cortex, CGE cells are mainly localized in layer 5, as seen when comparing (**g**) Nissl staining, (**h**) section *in situ* with *Etv1* (also known as *Er81*), which labels neurons in layer 5, and (**i**) alkaline phosphatase staining of cortical neurons. (**i**–**q**) Morphologies of CGE-derived neurons stained for alkaline phosphatase. In the cortex, CGE cells differentiated mainly into (**i**–**k**) stellate neurons, (**j**) where a projection to the MZ could be seen in a few cases. In the hippocampus, the majority of cells had (**l**) a spindly morphology, but (**m**) mossy and (**n**) pyramidal cells were also observed. Other morphologies included: (**o**) medium spiny neurons in the striatum, (**p**) aspiny neurons in the amygdala and (**q**) bipolar neurons in the nucleus accumbens. A, amygdala; DG, dentate gyrus; GP, globus pallidus; OT, olfactory tubercle; PIR, piriform cortex; SEP, septum; VP, ventral pallidum. Scale bars, (**a**–**f**) 500 μm, (**g**–**i**) 100 μm, (**j** and **m**) 125 μm, (**k**) 200 μm and (**l** and **n**–**q**) 40 μm.

may in fact be the largest source of hippocampal interneurons (**Figs. 5c–f, l, m** and **6d, f**). The MGE also contributed many cells to the hippocampus, which are mostly restricted to the CA1 region[24] (**Fig. 6e** and **g**). Consistent with previous results[24], LGE-derived cells did not contribute to the hippocampus (data not shown). CGE-transplanted cells also migrated tangentially to the cortex (**Figs. 5a–k** and **6h**), although more predominantly at posterior levels. Whereas both the MGE and CGE-derived cells migrated to the deeper layers of the cortex, the CGE contributed fewer cells and, as noted above, these were almost completely restricted to cortical layer 5 (**Figs. 5g–i** and **6h**). Brains receiving either MGE or CGE grafts were also found to have significant numbers of cells in the marginal zone (MZ). In CGE-grafted animals, the MZ also contained numerous axonal fibers, at least in part emanating from the layer-5 neurons. Both the CGE and MGE contributed cells to the amygdala, but interestingly, to a large extent, these cells populated different nuclei in a complementary fashion (**Fig. 6j–l**). In contrast, the LGE did not contribute to this region (**Supplementary Table 1** and data not shown). CGE-derived cells mainly contributed cells to the central nucleus, basomedial and medial nuclei of the amygdala and, to a lesser extent, to the cortical nucleus (**Fig. 6j**). CGE-derived cells were not observed in the lateral or basolateral nuclei of the amygdala. In contrast, MGE-derived cells migrated mainly to the lateral and basolateral nuclei (**Fig. 6k** and **l**). Only in the cortical amygdala nucleus was overlap between MGE and CGE-derived cells observed.

In summary, the *in vivo* fate maps presented here show that the three embryonic ganglionic eminences contribute to different structures in the adult brain. Although the CGE contributes to some regions in common with the MGE and LGE, it contributes to others that are distinct. Moreover, even in cases where two eminences contributed to a common structure, there was a differential distribution of cells within that structure.

Heterotopic transplantation of the MGE to the CGE

To determine whether the local environment or the site of origin of the grafted cells controls the pattern of migration, we transplanted MGE cells to the CGE. At P21, MGE cells that were heterotopically transplanted to the CGE at E13.5 migrated to the cortex in a pattern similar to that of MGE homotopic transplants (**Fig. 7b** and **c**; **Supplementary Table 1**), rather than CGE homotopic transplants (**Fig. 7a**). Additionally, heterotopic transplantation had no obvious effect on the specific amygdala nuclei to which MGE cells contributed (**Fig. 7c**). Hence, placing MGE cells in a more posterior location than their origin did not significantly change their pattern of migration. These results suggest that MGE and CGE cells have intrinsically different migratory properties that are specified by E13.5.

CGE cells are interneurons and striatal spiny neurons

We used immunohistochemical analysis with several neuronal markers to determine the phenotype of cells in adult brains from homotopic transplants (Methods; **Fig. 8**). Roughly 29% ($n = 73$ cells) of CGE-derived cells expressed GABA (**Fig. 8a–c**). In addition to their expression of GABA, interneurons can be subdivided according to their expression of calbindin, somatostatin, parvalbumin and calretinin[31–33]. Of the cells derived from the CGE, 17% ($n = 105$) were calbindin-positive (**Fig. 8d–f**), 27% ($n = 200$) were somatostatin-positive (**Fig. 8g–i**) and only 2.8% ($n = 179$) expressed parvalbumin (**Fig. 8j–o**). Although cells derived from the MGE gave rise to similar percentages of both somatostatin (26%; $n = 116$) and calbindin-positive (13%; $n = 143$) cells, the MGE gave rise to a higher percentage (30%; $n = 110$) of parvalbumin-positive cells (data not shown). Notably, neither the CGE ($n = 1$ of 109 cells) nor the MGE ($n = 0$ out of 45 cells; see also ref. 24) gave rise to many interneurons expressing calretinin (data not shown). Of the CGE-derived cells found within the striatal complex, 29% ($n = 35$ cells) expressed DARPP32, a marker of medium spiny projection neu-

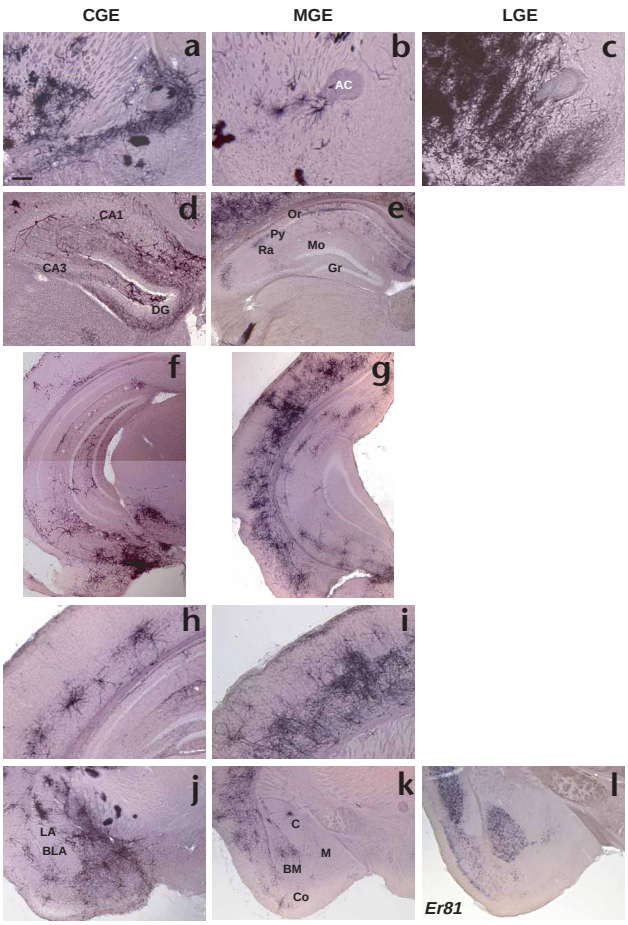

Fig. 6. Comparison of the differential contribution of CGE, MGE and LGE-derived cells to the cortex and limbic system. Coronal sections of P21 (**a**, **d**, **f**, **h**, **j**) CGE, (**b**, **e**, **g**, **i**, **k**) MGE and (**c**) LGE transplanted brains. Both (**a**) CGE and (**c**) LGE contribute to the nucleus accumbens, but at posterior and anterior levels, respectively. (**b**) MGE contributes only a few cells to this structure. (**d**, **f**) The CGE and (**e**, **g**) MGE contribute to the hippocampus at anterior and posterior levels. Likewise, both the (**h**) CGE and (**i**) MGE give rise to cortical neurons, though the MGE contributes to the cortex to a much higher extent. Similarly, (**j**) CGE and (**k**) MGE contribute to specific nuclei of the amygdala but in a generally complementary way. (**l**) Expression of *Etv1* in the amygdala marks nuclei contributed by the MGE. AC, anterior commissure. Hippocampal layers: Gr, granule; Mo, molecular; Or, oriens; Py, pyramidal; Ra, radiatum. Nuclei of the amygdala: BLA, basolateral; BM, basomedial; C, central; LA, lateral; M, medial. Scale bar (**a**–**e**), 200 μm; (**f**–**k**) 300 μm.

rons[34] (**Fig. 8p–r**). In contrast, the CGE, similar to the MGE and LGE, does not seem to be a major source of cortical excitatory pyramidal neurons. None of the CGE-derived cells expressed *Tbr1* ($n = 33$ cortical cells), which marks excitatory cortical neurons[35], and projection axons were not observed from PLAP-stained cortical cells (Methods). These results indicate that the CGE is source of interneurons that disperse throughout the telencephalon. For additional results, see **Supplementary Results** online.

also found that the CGE contributes to various regions of the basal limbic system and a subset of cortical and hippocampal interneurons in a pattern distinct from either the MGE or LGE. Hence, while all ventral telencephalic regions share in the expression of specific genes such as *Dlx2* and *Ascl1*, and produce cells that are able to undergo long-range tangential migration, each ganglionic eminence has a unique identity. Furthermore, at least with regard to their migratory behavior, progenitors from each of these regions are intrinsically programmed.

Previous work shows that the MGE and the LGE provide progeny to unique sets of telencephalic structures[24]. Here we found that CGE cells also populate specific territories in the mature brain, apart from those with cells of MGE or LGE origin. Strikingly, even though there is overlap in the structures populated by all three ganglionic eminences, the nuclei populated by the progeny from each eminence are distinct. Despite their different distributions, both morphological and immunocytochemical analyses suggest that these populations are interneurons. In addition, the CGE generates a large population of striatal projection neurons, previously thought to be derived solely from the LGE[36]. Our immunocytochemical analysis revealed that interneurons originating in the MGE versus CGE produced significantly different numbers of parvalbumin neurons, suggesting that these populations vary in their neurochemical profiles. However, limitations in the sensitivity of the PLAP antibody, which was used to detect donor cells, somewhat compromised our ability to fully characterize the phenotypes of mature CGE-derived cells. Hence,

Discussion

Here we examined both the potential and fate of cells originating within the CGE. This analysis revealed that rather than simply being a posterior extension of the MGE or LGE, the CGE is a progenitor region possessing a distinct identity. At present, no single gene exclusively marks the CGE, and there is no genetic mutation that specifically affects the CGE; we therefore relied on a combination of genetic loss-of-function, *in vitro* migration and *in vivo* fate-mapping approaches to study the potential uniqueness of this structure. Although it shares markers with both the MGE and LGE, the CGE's molecular and migratory properties as revealed by genetic loss-of-function analysis are unchanged in mutant mice that show abnormal development of the LGE or MGE. Using *in vivo* fate-mapping analysis, we

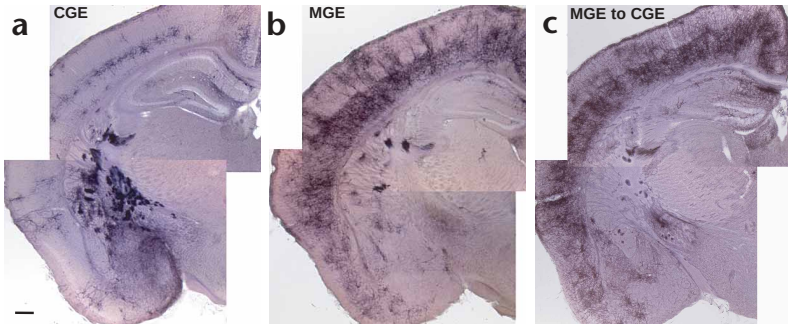

Fig. 7. MGE cells do not adopt CGE characteristics when transplanted to the more posterior CGE. (**a**–**c**) Coronal sections at P21 of (**a**) CGE-to-CGE, (**b**) MGE-to-MGE and (**c**) MGE-to-CGE transplanted brains. The heterotopic grafting of (**c**) MGE cells into the CGE did not change the migratory profile of the MGE cells, as they behaved more similarly to (**b**) MGE homotopic transplantations than (**a**) CGE homotopic transplantations. Scale bar (**a**–**c**), 300 μm.

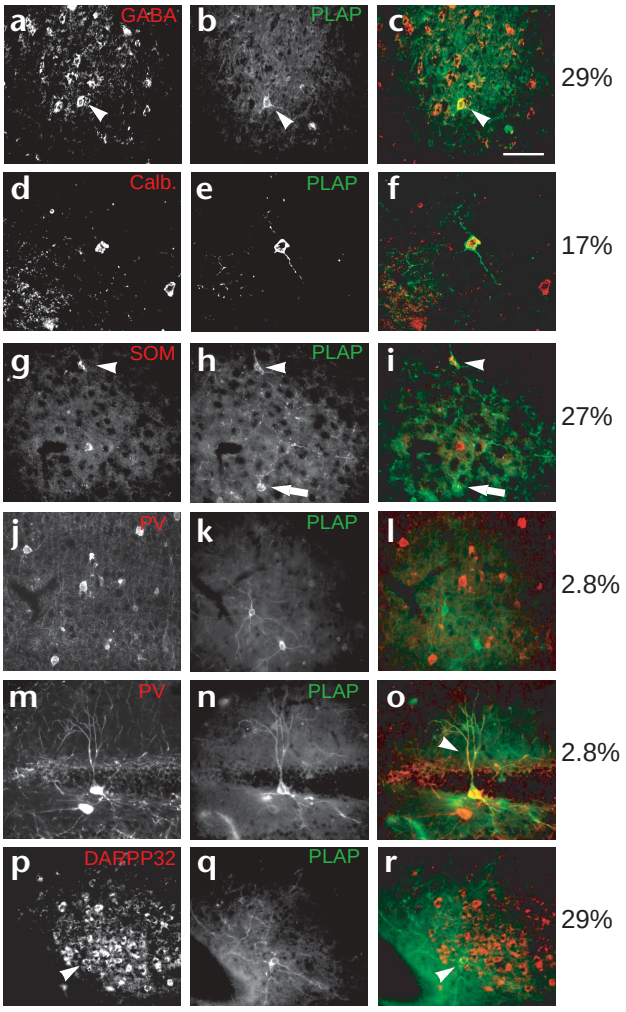

Fig. 8. Immunohistochemical characterization of CGE-derived cells. Postnatal cellular fates of transplanted cells are shown. Sections were double-labeled with antibodies against (**a**) GABA, (**d**) calbindin, (**g**) somatotstatin, (**j**, **m**) parvalbumin and (**p**) DARPP32 to identify cell type and with antibodies against (**b**, **e**, **h**, **k**, **n**, **q**) PLAP to identify transplanted cells. In each column, the left panel shows immunolabeled cells for each cell type marker. The center panel shows PLAP-positive cells in the same section. The right panel shows the overlay of the two images with the cells expressing specific cell type markers shown in red, PLAP positive cells in green (arrows) and double-labeled cells and cellular processes in yellow (arrowheads). Percentage of double-labeled cells for each marker is shown on the right. Images shown are from the (**a**–**l**) cortex, (**m**–**o**) dentate gyrus of the hippocampus and the (**p**–**r**) ventral pallidum. Scale bar, 50 μm.

it remains to be determined the extent to which cells of the same neuronal class originating from each of the eminences are of identical subtypes. Further insights into the diversity of these populations should come from future studies using a combination of immunocytochemical and electrophysiological methods.

Owing to the current lack of CGE-specific gene markers, it is important to note that our definition of the CGE at present is solely morphology-based. We defined the CGE as the region that is posterior to the fusion of the MGE and LGE. As the CGE is not separated from the MGE and LGE by a sulcus, it is not as clearly demarcated as the MGE or LGE. Despite the difficulty in defining this region, an array of experimental evidence including genetic loss-of-function, *in vitro* migratory assays and *in vivo* fate-mapping analysis supports the idea that this progenitor region is distinct from both the MGE and LGE.

The CGE may, however, be a heterogeneous structure comprised of subdomains that have distinct cellular and migratory fates. Indeed, the expression of *Titf1*, *Lhx6* and *Ebf1* in only a subset of anterior-most CGE cells suggests that this may be the case. For example, perhaps the common areas populated by cells from multiple eminences are a result of the overlap of genes expressed in the CGE and the MGE (for example, *Lhx6* and *Titf1*) or LGE (*Gsh2, Dlx2* and *Ebf1*). Conversely, migration from the CGE to regions of no or minimal overlap with MGE or LGE may be derived from the *Titf1*/*Lhx6*/*Ebf1*-negative region of the CGE. In this regard, the CGE, similar to the LGE, may ultimately prove to be comprised of a number of distinct subdomains. In the LGE, the dorsal-most aspect of this structure (the region at the cortical-striatal sulcus) expresses a number of dorsal markers, suggesting that this region is not of ventral origin but instead is an extension of the pallium[3,37,38]. Despite this heterogeneity, the LGE is still considered a single structure. Perhaps similarly, the discovery of new markers will help further delineate the CGE and allow the subdivisions within this structure to be better defined.

Irrespective of their grafted position, progenitors from the MGE and CGE maintain characteristic patterns of tangential migration. Specifically, MGE cells grafted into the CGE, as well as LGE cells transplanted to the MGE[24], continue to migrate according to their site of origin. Hence anterior-posterior positional identity is intrinsically determined within the ventral telencephalon by E13.5.

Here, and in a previous fate-map study of the ventral ganglionic eminences[24], the localization of MGE- and CGE-derived cells was restricted to the deeper layers of the cortex. Previous work has also shown that radial migrating cortical cells invade the developing cortex in an inside-out manner[39]. Furthermore, it has been shown that the laminar fate of migrating cortical cells is determined just before the last cell division[40]. Therefore, if our transplants captured cells at this time point (E13.5) in development, perhaps this is why they were restricted to deeper cortical layers. This may also explain the surprising paucity of ventrally derived cells that populate the globus pallidus or give rise to cortical oligodendrocytes.

It will be interesting to determine if transplants obtained from different time points of development generate cells of different migratory and cellular fates, and if, similar to radial migrating cortical cells, these putative differences are dependent on the cell cycle. Temporal issues aside, our results show that regional diversity in the ventral telencephalon must be broadened to include the CGE. Indeed, this study provides the first genetic, molecular and cellular insights into the CGE.

Methods

Animals and surgery. We used Swiss Webster (Taconic, New York) or CD1 (Charles River, Massachusetts) mice and maintained them according to protocols approved by the Institutional Animal Care and Use Committee at the New York University School of Medicine. The ultrasound scanner (UBM 840 scanner, Humphrey Instruments, San Leandro, California) was used as previously described[41].

Generation of *Dlx2-tau-lacZ* mice. A *tau-lacZ* targeting construct containing an upstream IRES (internal ribosome entry site) sequence and a downstream floxed *Neo* selection gene was inserted into the *Asc*I site of the third exon of the *Dlx2* gene. Genomic DNA isolated from selected

embryonic stem cells was cut with *Hin*dIII and probed with a *Xho*I-*Hin*dIII fragment from the 3′ region of the *Dlx2* locus. The *Neo* gene was excised by crossing heterozygous *Dlx2-tau-lacZ* mice to *NLS-Cre* transgenic mice. Heterozygous *Dlx2-tau-lacZ* transgenic mice are phenotypically indistinguishable from their wild-type littermates. For subsequent genotyping, we used X-gal staining on either whole embryo bodies or a toe clip, as previously described[12].

Genotyping of mice. The presence of the *PLAP* gene (codes for placental alkaline phosphatase) was detected by histochemical staining of the tails of pups or bodies of the embryos. Only embryos containing the transgene were used in the transplantation experiments. *Gsh2*$^{-/-}$ and *Titf1*$^{-/-}$ mice were genotyped as described[12,20].

Tissue preparation, histology, anatomy and *in situ* hybridization. Tissue samples were prepared as previously described[20]. A number of P21 samples were also cut coronally into 50–100 µm thick sections using a Vibratome (Leica). These animals were perfused with 4% PFA (paraformaldehyde) and 0.1% glutaraldehyde. Sections were used for histochemical detection of PLAP, for RNA *in situ* analysis or for immunofluorescence. Anatomical locations and projection pathways were determined by referring to previous work[42,43]. Whole-mount and section *in situ* hybridizations were carried out as described[44,45]. The cDNA probes that we used were *Dlx2*, *Ascl1*, *Titf1*, *Sfrp2*, *Neurog2*, *Lhx6*, *Ebf1* and *Etv1*.

Immunohistochemistry. Histochemical detection of PLAP and immunofluorescence were performed as described[46]. We used the following antibodies: rabbit anti-CRBP (1:200), sheep anti-PLAP (1:100, American Research Products, Belmont, Massachusetts), rabbit anti-PLAP (1:100, Accurate Chemical, Westbury, New York), rabbit anti-GABA (1:1,000, Sigma), rabbit anti-neurofilament-145 (1:1,000, Chemicon, Temecula, California), rabbit anti-somatostatin (1:2,500, Calbiochem, San Diego, California), mouse anti-parvalbumin (1:1,000, Sigma), rabbit anti-calretinin (1:500, Chemicon), rabbit anti DARPP-32 (1:1,000, Chemicon), rabbit anti-calbindin (1:1,000, Calbiochem) and rabbit anti-Tbr1 (1:100).

Secondary antibodies were from Jackson ImmunoResearch Laboratories (West Grove, Pennsylvania) and raised in donkeys. Fluorescent images were obtained using a cooled-CCD camera (Princeton Scientific Instruments, New Jersey) and Metamorph software (Universal Imaging, Downingtown, Pennsylvania). For quantification of double-labeled cells, only PLAP-labeled flourescent cells in which there was an obvious cell body were counted. Cells localized to the site of putative needle injection were excluded from the counting. Owing to the limitations of the GABA antibody, which only very weakly stained cells of the striatum, transplanted cells in the striatum were also excluded from the quantification of GABA-labeled cells. For immunohistochemical analysis, 5–10 CGE-to-CGE and 3–4 MGE-to-MGE brains were used.

Tissue dissection, culture conditions and quantification of Matrigel explants. VZ and SVZ from MGE, LGE, CGE and dorsolateral cortex were dissected from E13.5 *Titf1*$^{-/-}$ and control littermates, and cultured in Matrigel (BD Biosciences, Bedford, Massachusetts) as described[20,30]. Quantification (**Fig. 3x**) was done by overlaying a 16-spoked grid on a picture of each explant and measuring the maximal distance of cell migration from the edge of the explant along each of the 16 points. Values for each explant were averaged and compared using a single-factor analysis of variance (ANOVA, $P < 0.002$), and significance between compared values was determined by a two-tailed Student's *t*-test.

Donor cell preparation for *in vivo* transplantation. VZ and SVZ from the ganglionic eminences of PLAP transgenic mice[47] were dissected from 8–15 mouse embryos (E13.5) and prepared as described[30]. The CGE was defined morphologically as the region posterior to the MGE/LGE sulcus and anterior to the most caudal cortex (*Neurog2*-negative). Tissue was dissected from the LGE and MGE above and below the sulcus that clearly divides these two regions.

***In utero* transplantation.** *In vivo* ultrasound-guided transplantations were performed as described[24]. We injected 20–40 nl of the cell suspension—corresponding to 15,000–30,000 cells—into the CGE, LGE or MGE of E13.5 hosts. Transplanted embryos were collected at 2 (data not shown) and 4 days after transplantation, or when they had grown to 3 week and 4–6 month old animals. For embryonic time points, 6 CGE-to-CGE, 4 MGE-to-MGE and 2 LGE-to-LGE brains were considered. For the P21 analysis, we included a total of 14 CGE-to-CGE, 4 MGE-to-MGE, 3 LGE-to-LGE and 4 MGE-to-CGE successfully transplanted animals.

Note: Supplementary information is available on the Nature Neuroscience website.

Acknowledgments

We thank the Fishell lab, H. Wichterle, J. Goldman and I. Zohn for critical reading and M. Rutlin and Y.Y. Huang for technical assistance. We thank A. Langston and E. Na for generating the Dlx2-tau-lacZ transgenic line and the following for their gifts of reagents: J.R. Stringer, A. Joyner, F. Guillemot, J. Rubenstein, J. Nathans, S. Arber, P. Charnay, U. Eriksson and M. Sheng. S.N. is supported by PRAXIS XXI through the Gulbenkian Ph.D. program and J.C. is a recipient of a NIH postdoctoral fellowship NS10962-03. This work was supported by a National Institutes of Health grant (RO1 NS39007-03) and a March of Dimes basic research grant to G.F.

Competing interests statement

The authors declare that they have no competing financial interests.

RECEIVED 6 AUGUST; ACCEPTED 8 OCTOBER 2002

1. Fentress, J. C., Stanfield, B. B. & Cowan, W. M. Observation on the development of the striatum in mice and rats. *Anat. Embryol. (Berl.)* **163**, 275–298 (1981).
2. Smart, I. H. M. and Sturrock, R. R. in *The Neostriatum* (eds. Divac, I. & Oberg, R.G.E.) 127–147 (Pergamon, Oxford, 1979).
3. Puelles, L. *et al.* Pallial and subpallial derivatives in the embryonic chick and mouse telencephalon, traced by the expression of the genes *Dlx-2*, *Emx-1*, *Nkx-2.1*, *Pax-6*, and *Tbr-1*. *J. Comp. Neurol.* **424**, 409–438 (2000).
4. Anderson, S. A., Eisenstat, D. D., Shi, L. & Rubenstein, J. L. Interneuron migration from basal forebrain to neocortex: dependence on *Dlx* genes [see comments]. *Science* **278**, 474–476 (1997).
5. Anderson, S. A., Marin, O., Horn, C., Jennings, K. & Rubenstein, J. L. Distinct cortical migrations from the medial and lateral ganglionic eminences. *Development* **128**, 353–363 (2001).
6. de Carlos, J. A., Lopez-Mascaraque, L. & Valverde, F. Dynamics of cell migration from the lateral ganglionic eminence in the rat. *J. Neurosci.* **16**, 6146–6156 (1996).
7. Lavdas, A. A., Grigoriou, M., Pachnis, V. & Parnavelas, J. G. The medial ganglionic eminence gives rise to a population of early neurons in the developing cerebral cortex. *J. Neurosci.* **19**, 7881–7888 (1999).
8. Pleasure, S. J. *et al.* Cell migration from the ganglionic eminences is required for the development of hippocampal GABAergic interneurons. *Neuron* **28**, 727–740 (2000).
9. Tamamaki, N., Fujimori, K. E. & Takauji, R. Origin and route of tangentially migrating neurons in the developing neocortical intermediate zone. *J. Neurosci.* **17**, 8313–8323 (1997).
10. Anderson, S.A. *et al.* Mutations of the homeobox genes *Dlx-1* and *Dlx-2* disrupt the striatal subventricular zone and differentiation of late born striatal neurons. *Neuron* **19**, 27–37 (1997).
11. Casarosa, S., Fode, C. & Guillemot, F. *Mash1* regulates neurogenesis in the ventral telencephalon. *Development* **126**, 525–534 (1999).
12. Corbin, J. G., Gaiano, N., Machold, R. P., Langston, A. & Fishell, G. The *Gsh2* homeodomain gene controls multiple aspects of telencephalic development. *Development* **127**, 5007–5020 (2000).
13. Marin, O., Anderson, S. A. & Rubenstein, J. L. Origin and molecular specification of striatal interneurons. *J. Neurosci.* **20**, 6063–6076 (2000).
14. Sussel, L., Marin, O., Kimura, S. & Rubenstein, J. L. Loss of *Wkx2.1* homeobox gene function results in a ventral to dorsal molecular respecification within the basal telencephalon: evidence for a transformation of the pallidum into the striatum. *Development* **126**, 3359–3370 (1999).
15. Toresson, H., Potter, S. S. & Campbell, K. Genetic control of dorsal-ventral identity in the telencephalon: opposing roles for *Pax6* and *Gsh2*. *Development* **127**, 4361–4371 (2000).
16. Yun, K., Potter, S. & Rubenstein, J. L. *Gsh2* and *Pax6* play complementary roles in dorsoventral patterning of the mammalian telencephalon. *Development* **128**, 193–205 (2001).
17. Corbin, J. G., Nery, S. & Fishell, G. Telencephalic cells take a tangent: non-radial migration in the mammalian forebrain. *Nat. Neurosci.* **4**, (Suppl.), 1177–1182 (2001).
18. Parnavelas, J. G. The origin and migration of cortical neurones: new vistas. *Trends Neurosci.* **23**, 126–131 (2000).

19. He, W., Ingraham, C., Rising, L., Goderie, S. & Temple, S. Multipotent stem cells from the mouse basal forebrain contribute GABAergic neurons and oligodendrocytes to the cerebral cortex during embryogenesis. *J. Neurosci.* **21**, 8854–8862 (2001).
20. Nery, S., Wichterle, H. & Fishell, G. Sonic hedgehog contributes to oligodendrocyte specification in the mammalian forebrain. *Development* **128**, 527–540 (2001).
21. Olivier, C. *et al.* Monofocal origin of telencephalic oligodendrocytes in the anterior entopeduncular area of the chick embryo. *Development* **128**, 1757–1769 (2001).
22. Perez Villegas, E. M. *et al.* Early specification of oligodendrocytes in the chick embryonic brain. *Dev. Biol.* **216**, 98–113 (1999).
23. Spassky, N. *et al.* Multiple restricted origin of oligodendrocytes. *J. Neurosci.* **18**, 8331–8343 (1998).
24. Wichterle, H., Turnbull, D. H., Nery, S., Fishell, G. & Alvarez-Buylla, A. *In utero* fate mapping reveals distinct migratory pathways and fates of neurons born in the mammalian basal forebrain. *Development* **128**, 3759–3771 (2001).
25. Olsson, M., Bjorklund, A. & Campbell, K. Early specification of striatal projection neurons and interneuronal subtypes in the lateral and medial ganglionic eminence. *Neuroscience* **84**, 867–876 (1998).
26. Kim, A. S., Anderson, S. A., Rubenstein, J. L., Lowenstein, D. H. & Pleasure, S. J. *Pax-6* regulates expression of SFRP-2 and *Wnt-7b* in the developing CNS. *J. Neurosci.* **21**, RC132 (2001).
27. Toresson, H., Mata de Urquiza, A., Fagerstrom, C., Perlmann, T. & Campbell, K. Retinoids are produced by glia in the lateral ganglionic eminence and regulate striatal neuron differentiation. *Development* **126**, 1317–1326 (1999).
28. Szucsik, J. C. *et al.* Altered forebrain and hindbrain development in mice mutant for the *Gsh-2* homeobox gene. *Dev. Biol.* **191**, 230–242 (1997).
29. Garel, S., Marin, F., Grosschedl, R. & Charnay, P. *Ebf1* controls early cell differentiation in the embryonic striatum. *Development* **126**, 5285–5294 (1999).
30. Wichterle, H., Garcia-Verdugo, J.M., Herrera, D.G. & Alvarez-Buylla, A. Young neurons from medial ganglionic eminence disperse in adult and embryonic brain. *Nat. Neurosci.* **2**, 461–466 (1999).
31. DeFelipe, J. Neocortical neuronal diversity: chemical heterogeneity revealed by colocalization studies of classic neurotransmitters, neuropeptides, calcium-binding proteins and cell surface molecules. *Cereb. Cortex* **3**, 273–289 (1993).
32. Gonchar, Y. & Burkhalter, A. Three distinct families of GABAergic neurons in rat visual cortex. *Cereb. Cortex* **7**, 347–358 (1997).
33. Kubota, Y., Hattori, R. & Yui, Y. Three distinct subpopulations of GABAergic neurons in rat frontal agranular cortex. *Brain Res.* **649**, 159–173 (1994).
34. Ouimet, C. C., Miller, P. E., Hemmings, H. C. Jr., Walaas, S. I. & Greengard, P. DARPP-32, a dopamine- and adenosine 3':5'-monophosphate-regulated phosphoprotein enriched in dopamine-innervated brain regions. III. Immunocytochemical localization. *J. Neurosci.* **4**, 111–124 (1984).
35. Hevner, R. F. *et al.* Tbr1 regulates differentiation of the preplate and layer 6. *Neuron* **29**, 353–366 (2001).
36. Olsson, M., Campbell, K., Wictorin, K. & Bjorklund, A. Projection neurons in fetal striatal transplants are predominantly derived from the lateral ganglionic eminence. *Neuroscience* **69**, 1169–1182 (1995).
37. Marin, O. & Rubenstein, J. L. A long, remarkable journey: tangential migration in the telencephalon. *Nat. Rev. Neurosci.* **2**, 780–790 (2001).
38. Schuurmans, C. & Guillemot, F. Molecular mechanisms underlying cell fate specification in the developing telencephalon. *Curr. Opin. Neurobiol.* **12**, 26–34 (2002).
39. Angevine, J. B. Jr. & Sidman, R. L. Autoradiographic study of cell migration during histogenesis of cerebral cortex in the mouse. *Nature* **192**, 766–768 (1961).
40. McConnell, S. K. & Kaznowski, C. E. Cell cycle dependence of laminar determination in developing neocortex. *Science* **254**, 282–285 (1991).
41. Liu, A., Joyner, A. L. & Turnbull, D. H. Alteration of limb and brain patterning in early mouse embryos by ultrasound-guided injection of Shh-expressing cells. *Mech. Dev.* **75**, 107–115 (1998).
42. Martin, J. H. *Neuroanatomy: Text and Atlas* (Elsevier, New York, 1989).
43. Paxinos, G. *The Rat Nervous System* (Academic, New York, 1995).
44. Schaeren-Wiemers, N. & Gerfin-Moser, A. A single protocol to detect transcripts of various types and expression levels in neural tissue and cultured cells: *in situ* hybridization using digoxigenin-labelled cRNA probes. *Histochemistry* **100**, 431–440 (1993).
45. Wilkinson, D.G. & Nieto, M.A. Detection of messenger RNA by *in situ* hybridization to tissue sections and whole mounts. *Methods Enzymol.* **225**, 361–373 (1993).
46. Gaiano, N., Kohtz, J. D., Turnbull, D. H. & Fishell, G. A method for rapid gain-of-function studies in the mouse embryonic nervous system [see comments]. *Nat. Neurosci.* **2**, 812–819 (1999).
47. DePrimo, S. E., Stambrook, P. J. & Stringer, J. R. Human placental alkaline phosphatase as a histochemical marker of gene expression in transgenic mice. *Transgenic Res.* **5**, 459–466 (1996).